Towards a rheological classification of flow induced crystallization experiments of polymer melts

Please check the document version of this publication:

• A submitted manuscript is the version of the article upon submission and before peer-review. There can be important differences between the submitted version and the official published version of record. People interested in the research are advised to contact the author for the final version of the publication, or visit the DOI to the publisher's website.
• The final author version and the galley proof are versions of the publication after peer review.
• The final published version features the final layout of the paper including the volume, issue and page numbers.

Link to publication

Jan van Meerveld
Gerrit W. M. Peters
Markus Hütter

Towards a rheological classification of flow induced crystallization experiments of polymer melts

J. van Meerveld (✉)
Institute of Polymers,
Department of Materials,
ETH, CH-8092 Zürich, Switzerland
E-mail: meerveld@mat.ethz.ch

G. W. M. Peters
Dutch Polymer Institute (DPI),
Section Material Technology (MaTe),
University of Technology Eindhoven,
Eindhoven, The Netherlands

M. Hütter
Department of Chemical Engineering,
Massachusetts Institute of Technology,
Cambridge, Massachusetts, USA

Abstract Departing from molecular based rheology and rubber theory, four different flow regimes are identified associated to (1) the equilibrium configuration of the chains, (2) orientation of the contour path, (3) stretching of the contour path, and (4) rotational isomerization and a deviation from the Gaussian configuration of the polymer chain under strong stretching conditions. The influence of the ordering of the polymer chains on the enhanced point nucleation, from which spherulites grow, and on fibrous nucleation, from which the shish-kebab structure develops, is discussed in terms of kinetic and thermodynamic processes. The transitions between the different flow regimes, and the associated physical processes governing the flow induced crystallization process, are defined by Deborah numbers based on the reptation and stretching time of the chain, respectively, as well as a critical chain stretch. An evaluation of flow induced crystallization experiments reported in the literature performed in shear, uniaxial and planar elongational flows quantitatively illustrates that the transition from an enhanced nucleation rate of spherulites towards the development of the shish-kebab structure correlates with the transition from the orientation of the chain segments to the rotational isomerization of the high molecular weight chains in the melt. For one particular case this correlation is quantified by coupling the wide angle X-ray diffraction and birefringence measurements of the crystallization process to numerical simulations of the chain stretch of the high molecular weight chains using the extended Pom-Pom model in a cross-slot flow.

Keywords Isotactic polypropylene · Molecular weight distribution · Polymer melts · Shish-kebab structure · Rotational isomerization

Introduction

Flow induced crystallization (FIC) experiments differ from each other with respect to (1) the polymer system, (2) the molecular weight distribution (MWD) of the melt, (3) the temperature T, at which the experiment is performed, (4) the flow type (shear, extensional or a mixed flow), and finally (5) the flow rate and total deformation applied on the sample. As a result of the large variation of experimental parameters it is difficult, first, to perform a fair comparison between different experiments and, second, to identify general trends and physical processes governing the FIC dynamics. The latter is important for the development of sound

physical FIC models and their validation against experiments. These difficulties are illustrated in two examples.

In the first example we discuss the validation of the models developed by Coppola et al. (2001) and Zuidema et al. (2001) against the experimental results of Lagasse and Maxwell (1976). The following three features of the model of Coppola et al. (2001) are of relevance here. First, a single average relaxation time is considered for the entire melt, second, only the average orientational order of the contour path (not the stretch) of the chains enhances the thermodynamic driving force, and finally, the reciprocal of the enhanced homogeneous nucleation rate of spherulites is used as a measure for the reduced induction time. In the model of Zuidema et al. (2001) the important model features are different. First, the formation of the shish-kebab structure is considered besides the heterogeneous nucleation of spherulites. Second, the critical parameter describing the formation of the shish is related to the recoverable strain and depends on both the orientation and the stretch of the chains. Third, the time needed to reach a critical crystallinity is considered to correlate to the induction time. Fourth, a multi-mode approach is taken for the rheological description. Anticipating that the high molecular weight (HMW) chains of the melt dominate the FIC only the mode with the longest relaxation times drives the formation of the shish-kebab structure. Finally, nuclei are assumed to act as physical cross-links which further increase the relaxation times of the HMW chains. Despite the relevant features in the models of Coppola et al. (2001) and Zuidema et al. (2001) differing in almost any aspect, the same experiment of Lagasse and Maxwell (1976) can still be described successfully. (The model of Zuidema et al. 2001 has also been confronted with other experimental protocols in simple shear, duct and cross-slot flows; Zuidema et al. 2001; Zuidema 2000; Peters et al. 2002; Swartjes 2001; Swartjes et al. 2003.) This indicates that the validation of these models against the experiment of Lagasse and Maxwell (1976) is still inconclusive with respect to the physical process governing the FIC dynamics.

As a second example we consider the generally assumed correlation between the development of the shish-kebab morphology and 'strong' chain stretching conditions (Mackley and Keller 1973; Keller and Kolnaar 1997) without quantifying the difference between 'weak' and 'strong' chain stretching. Nevertheless the shish-kebab morphology develops in both extensional and shear flows (Keller and Kolnaar 1997; Eder and Janeschitz-Kriegl 1997) although the latter is generally referred to as a 'weak' flow, as stretching of the chain is more difficult (Astarita 1979; Larson 1988). Recent molecular dynamic simulations show that the shish structure develops provided the PE chain is in the all-trans (zig-zag) conformation (Dukovski and

Muthukumar 2003; Lavine et al. 2003). The latter implies that the chain is (locally) stretched to the maximum extend, but does not resolve the quantitative difference between 'weakly' and 'strongly' stretched chains.

The purpose of this paper is to identify different flow regimes associated to specific degrees of ordering of the polymer chains with the goal of gaining a general understanding (classification) of which physical processes govern the FIC dynamics. The influence of the different chemical structures of polymer systems, the tacticity and the stereoregularity of the chains on the crystallization dynamics is not addressed or analyzed. The paper is organized as follows. First, the different flow regimes are identified. Second, the influence of a specific flow regime on the FIC dynamics is discussed. Third, the correlation between the different flow regimes and the changes in the crystallization dynamics is illustrated for FIC experiments in shear and extensional flows. Fourth, the different procedures to characterize the flow regimes are evaluated, given the importance in the analysis of a given experiment. Finally, conclusions are drawn.

Molecular based rheological modeling

In molecular based rheological models, such as the Doi-Edwards model (Doi and Edwards 1986) and its extensions, see for example Mead and Leal (1995), Mead et al. (1998), Fang et al. (2000), Watanabe (1999), and McLeish (2002)], a flexible polymer chain is represented by the contour path. This contour path is a smoothed curve through the actual atomistic configuration of the backbone of a particular polymer chain; see Fig. 1. Dynamic equations are formulated for the orientation vector of unit length, u, along the contour path and the stretch ratio, λ. The stretch ratio is defined as the ratio of the current length of the contour path, L, to the equilibrium value, L_0, $\lambda = L/L_0$. For the rheological description it is important to distinguish two timescales. First, the reptation time, τ_{rep}, associated with the reptation process and the orientation vector u and, second, the time scale τ_s for the faster chain retraction and the stretch ratio λ. For monodisperse melts these two time scales are related to each other via the relationship $\tau_{rep}/\tau_s = 3Z(1 - 1.51/\sqrt{Z})^2$ (Doi and Edwards 1986; Ketzmerick and Öttinger 1989) with Z the number of entanglements per chain. As $Z > 100$ for typical polymer melts the magnitude of τ_{rep} and τ_s are separated by at least two orders of magnitude. This observation directly implies that the contour path can be orientated at much lower flow rates compared to those required to stretch it. This is conveniently expressed by two Deborah numbers for shear and extensional flow, De, based on τ_{rep} and τ_s, defined as

$$De_{rep} = a_\tau \tau_{rep} \dot{\gamma}, a_\tau \tau_{rep} \dot{\varepsilon} \tag{1}$$
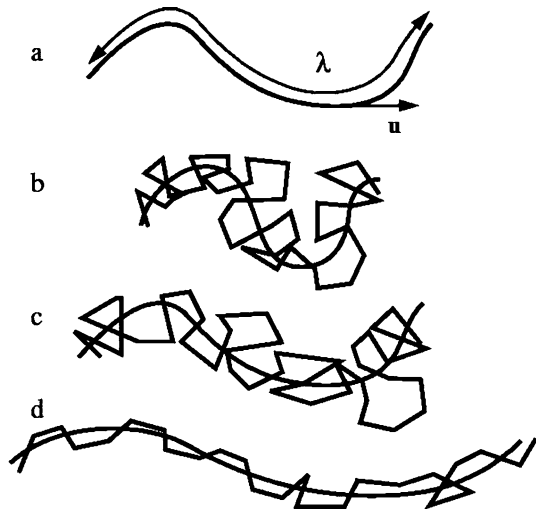
Fig. 1 a Sketch of the contour path of a chain and the physical meaning of the orientation vector **u** of a segment on the contour path and the average chain stretch λ. **b–d** Sketch of the contour path (*smoothed curve*) and the Kuhn chain at equilibrium; (b) De_{rep}, $De_s < 1$, $\lambda = 1$, for an oriented but non-stretched contour path; (c) $De_{rep} > 1$, $De_s < 1$, $\lambda = 1$, for an oriented and stretched contour path; (d) $De_{rep}, De_s > 1$, $\lambda > 1$

$$De_s = a_\tau \tau_s \dot{\gamma}, a_\tau \tau_s \dot{\varepsilon} \qquad (2)$$

with $\dot{\gamma}$ the shear rate, $\dot{\varepsilon}$ the extension rate and a_τ the time-temperature shift factor (Macosko 1996), respectively.

In the flow regime $1/\tau_{rep} < \dot{\gamma}, \dot{\varepsilon} < 1/\tau_s$ the relaxation dynamics known as convective constraint release, CCR (Marrucci 1996; Ianniruberto and Marrucci 1996) is essential in the understanding and prediction of the rheological behavior of a polymer melt: see, for example, Mead et al. (1998) and Fang et al. (2000). The effect of CCR enhances the orientational relaxation dynamics in an approximately linear fashion with the strain rate. As a consequence the orientational ordering of the chain is arrested to a specific magnitude. This is confirmed experimentally in shear flows, where it is observed that the orientation angle is approximately equal to about 20 degrees (depending on the number of entanglements per chain) for $1/\tau_{rep} < \dot{\gamma}, \dot{\varepsilon} < 1/\tau_s$ (Islam and Archer 2001; Islam et al. 2003; Oberhauser et al. 1996).

If the chain is stretched, two different regimes can be identified based on the global configuration of the chain and the rotational isomerization (RI) at temperatures well above the melting temperature, T_m (Abe and Flory 1970; Treloar 1975; Flory 1989). For small λ, the chain maintains a Gaussian configuration (Treloar 1975; Flory 1989) and the amount of RI is small (Abe and Flory 1970). At large λ, the influence of the finite extensibility of the chain sets in and the chain configuration becomes non-Gaussian (Treloar 1975; Flory 1989) and the amount of RI is large (Taylor et al. 1999; Cail et al. 2000). The parameter λ^* denotes the transition between

the two chain stretching regimes, which may be identified as weak and strong stretching conditions respectively. For $T > T_m$ the approximate magnitude of λ^* may be obtained from the relationship (Treloar 1975)

$$\lambda^*/\lambda_{max} = \alpha \qquad (3)$$

Values of α are discussed below and λ_{max} is the maximum extension ratio. Assuming a Gaussian configuration of the chain at equilibrium, the magnitude of λ_{max} equals (Flory 1989; Fang et al. 2000)

$$\lambda_{max} = \sqrt{N_K} = \frac{b}{l_K} = \frac{b}{l(C_\infty + 1)} \qquad (4)$$

with N_K the average number of Kuhn segments per entanglement, b the tube diameter, l_K the Kuhn length, l the bond length, and C_∞ the characteristic ratio representing the stiffness of the polymer chain (Flory 1989). The universal behavior suggested by Eq. (3), which is directly related to the universal behavior of the inverse Langevin probability of the chain, is only valid in the limit of a large number of Kuhn segments, $N_K \to \infty$ (Treloar 1975; Flory 1989). In real polymer systems the magnitude of N_K is small and the exact probability distribution shows that the deviation from the Gaussian configuration has a non-universal dependency on N_K (Sect. 6.6 of Treloar 1975); Chap. 8 of Flory 1989). As a result, the parameter α is a decreasing function of N_K and reaches the magnitude of about 1/3 in the limit of $N_K \to \infty$ to indicate a deviation from the Gaussian configuration of the chain. Reducing the temperature T towards T_m gives an increase of the chain stiffness, i.e., C_∞ increases for decreasing T (Flory 1989; Dressler 2000). In addition, a homogeneous distribution of the conformations can be questioned for $T < T_m$ (Flory 1989; Lavine et al. 2003). This has two consequences. First, the magnitude of λ^* is temperature dependent, $\lambda^* = \lambda^*(T)$, and decreases with decreasing T. Second, the connection between λ and the conformation of the chain segments is, for $T < T_m$, less direct compared to $T > T_m$ (as the conformation is affected by both the T and chain stretching for $T < T_m$). From the difficulties in quantifying the influence of N_K and T on the magnitude λ^*, the expression $\lambda^*/\lambda_{max} = \alpha(N_K, T)$ should (perhaps) be regarded as a (semi-)empirical relationship, serving to indicate qualitative trends on the change of the configuration and conformation of the chain upon chain stretching at a given temperature. Nevertheless, for small undercooling it is assumed that the two chain stretching regimes can be identified, just as for $T > T_m$, and will be used hereafter.

It is important to distinguish between the orientation of the contour path, as used in the formulation of the rheological models, and the orientation of the Kuhn segments. The latter can be obtained using birefringence or FTIR measurements and is often used to explain the

influence of the flow on the crystallization. In uniaxial elongation flows the Hermans orientation factor of the Kuhn segments, P_2, is often analyzed, which is the ratio of the current to the maximum birefringence of the melt. In that case P_2 can be expressed in terms of λ and $\boldsymbol{u}$ as (Mead and Leal 1995; Strobl 1997)

$$P_2 = \left[\frac{3}{5} \left(\frac{\lambda}{\lambda_{\max}} \right)^2 + \frac{1}{5} \left(\frac{\lambda}{\lambda_{\max}} \right)^4 \right.$$
$$\left. + \frac{1}{5} \left(\frac{\lambda}{\lambda_{\max}} \right)^6 \right] \left(\langle \boldsymbol{uu} \rangle_{xx} - \langle \boldsymbol{uu} \rangle_{yy} \right) \tag{5}$$

with $\langle \boldsymbol{uu} \rangle$ the average second order orientation tensor of the contour path and x and y denote the component parallel and perpendicular to the elongation direction. The expression for P_2 directly shows that the orientation of the Kuhn segments is enhanced due to both the orientation and stretch of the contour path and hence governed by both the magnitude of De_{rep} and De_s. This is illustrated in Fig. 1 where it should be noted that the fluctuation of the Kuhn chain around the contour path remains identical to equilibrium for $De_s < 1$.

In the above, a monodisperse melt is implicitly considered despite the fact that polydisperse melts are used in most experimental investigations. Moreover, there is strong experimental evidence that the HMW tail of the MWD dominates the FIC dynamics (Vleeshouwers and Meijer 1996; Nogales et al. 2001; Kumaraswamy et al. 2002; Seki et al. 2002; Kornfield et al. 2003). Consequently, the question arises if the different flow regimes identified above can be applied directly to the HMW tail or does the polydispersity of the particular polymer melt influence the ordering of the chains in, and the transitions between, the different regimes in the weak shear and strong uniaxial flows? A molecular based rheological model for polydisperse melts is developed to address this question from a theoretical viewpoint (van Meerveld 2004a). For further details the reader is referred to the original paper. Here, only the influence of the mass fraction of the HMW chains, ϕ, and the ratio of the molecular weight of the HMW chains, M_{HMW}, to the weight averaged molecular weight of the melt, M_W, i.e., M_{HMW}/M_W, on the orientation and stretch of the contour path of the HMW chains is summarized. In this setting the polydisperse melt is crudely modeled as a bidisperse system of chains with a HMW and an average molecular weight respectively. For $\phi < 0.1$ a variation of ϕ on the orientation and chain stretch is small as the 'tube' around the HMW chains is primarily formed by the LMW chains. Keeping M_{HMW} fixed, i.e., De_{rep} and De_s of the HMW chains remain constant, and increasing M_{HMW}/M_W changes the ordering of the HMW chains from two aspects. First, it becomes more difficult to orient the HMW chains into the flow direction of both shear and uniaxial flows. Second, the chain stretching in

shear flows is affected by the MWD, due to the sensitive coupling of the chain stretching dynamics with the orientation of the chains in the flow field. (For a more detailed discussed the reader is referred to van Meerveld 2004a.) For 'moderate' values of M_{HMW}/M_W the reduced orientational ordering of the chain results into an increased ability to stretch the HMW chain. Consequently, the chains are stretched to a larger extend for a given De_s with increasing M_{HMW}/M_W. Hence, the requirement $\lambda > \lambda^*(T)$ is fulfilled more easily with increasing M_{HMW}/M_W. For 'large' M_{HMW}/M_W one may reach the condition that the HMW chains become 'too' weakly aligned into the flow field and the ability to stretch the HMW chain reduces with a further increase of M_{HMW}/M_W. For a given De_s the HMW chain stretch can be larger compared to $M_{\text{HMW}}/M_W = 1$, but may be smaller compared to that of a melt of 'moderate' M_{HMW}/M_W. Due to the influence of the MWD on the chain stretching dynamics in shear flows the condition $\lambda > \lambda^*(T)$ cannot be related to a single universal magnitude for De_s, but depends on the particular MWD of the melt in hand. A quantitative definition of 'moderate' and 'large' M_{HMW}/M_W cannot be identified based on the analysis in van Meerveld (2004a). Stretching of the HMW chains in uniaxial flows is primarily dominated by M_{HMW} and weakly influenced by M_{HMW}/M_W and the condition $De_s > 1$ indicates the relative sharp transition towards $\lambda > \lambda^*(T)$.

Summarizing the above, the influence of the flow can be separated into four regimes. For De_{rep}, $De_s < 1$ the chains are at equilibrium, i.e., the contour path is randomly oriented and not stretched. Subsequently three transitions are identified corresponding to increasing orientational order of the contour path with $De_{\text{rep}} > 1$, the onset of chain stretching with $De_s > 1$, and finally the onset of RI affecting the conformation as well as a deviation from the Gaussian configuration of the polymer chain, $\lambda > \lambda^*(T)$. The MWD of the melt influences the ordering of the HMW chains in two aspects. For a given M_{HMW} of the HMW chains and increasing M_{HMW}/M_W, first, the orientation order of the HMW chains reduces for $De_{\text{rep}} > 1$, $De_s < 1$ in shear and uniaxial flows, and, second, in shear flows the condition $\lambda > \lambda^*(T)$ cannot be related to a single value of De_s, as the chain stretching dynamics are influenced by the MWD.

Phase change dynamics

The change in order between the amorphous melt at $T > T_m$ and the crystalline phase can be specified by means of order parameters associated to (1) the density, (2) the periodic, crystallographic, ordering of the segments, (3) the orientational order of the chain segments, similar to P_2, and (4) the change in conformational order

of the chain segments. From the previous section it is expected that the application of the flow field will primarily affect the last two order parameters, i.e., the orientation and the conformation of the chain segments. As a consequence of the four different order parameters the nucleation process is expected to be of substantial complexity and not amenable to models based on a single pathway.

In discussing the influence of the applied flow field on the FIC we distinguish between the kinetic and the thermodynamic processes as reflected, for example, in the classical nucleation theory (Oxtoby 1992; Debenedetti 1996; Gunton 1999). The kinetic contribution represents the time scale for nucleation, the 'prefactor', and the thermodynamic contribution is associated to the position of the system in the (dynamic) phase diagram.

First the kinetic contribution is discussed. Under quiescent conditions, De_{rep}, $De_s < 1$, a nucleus is formed after a critical fluctuation in one, or more, order parameters. The nucleation process is purely stochastic in nature under these conditions. For $De_{rep} > 1$, $De_s < 1$, the chain segments become more uniformly oriented in the flow direction but the conformation remains unaffected. Hence, only a fluctuation in the conformation can be sufficient for the development of a nucleus. It should be noted that due to the CCR mechanism, as well as the polydisperse nature of the melt, the orientational ordering of the (HMW) chains is arrested to a specific magnitude (as reflected by an approximately constant orientation angle for $1/\tau_{rep} < \dot{\gamma} < 1/\tau_s$ as discussed above). This argument is supported by SANS measurement in shear flow (Muller and Picot 1992; Muller et al. 1993), which reveal that the deviation from the spherical coil conformation is rather weak and limited to a certain extent for $1/\tau_{rep} < \dot{\gamma} < 1/\tau_s$. The latter is in agreement with model predictions (McLeish 2002). The deviation from the spherical coil configuration is proposed to be the primary mechanism to drive flow induced crystallization by Nogales et al. (2001). In view of the arrested orientational order for $De_s < 1$ this mechanism is rather limited in this flow regime. Under fast flowing conditions, De_{rep}, $De_s > 1$, $\lambda > \lambda^*(T)$, one reaches the condition where the chain segments are strongly oriented and the chain conformation becomes similar to that of the crystalline state. As a consequence, critical fluctuations in the orientation and conformation of the chain segments are no longer required as these conditions are fulfilled, in a deterministic manner, during the flow. The application of the flow field therefore shifts the nucleation dynamics from a stochastic to a more deterministic process, resulting in an increase of the observed nucleation rate.

Second, the change in the thermodynamic contribution is discussed. Following the pioneering work of Flory (1947), the thermodynamic driving force can be enhanced by the flow field, which is reflected by an effective increase in T_m. Under quiescent conditions the temperature governs the thermodynamic driving force, which is then enhanced due to the orientational and stretching of the (HMW) chains depending on the particular flow regime. This is an essential feature in the model of Coppola et al. (2001) and strain induced crystallization models of rubbers (Flory 1947), although the importance, based on a description of the chains on a macroscopic level, is questioned by McHugh et al. (1993) and Janeschitz-Kriegl et al. (2003).

For a number of polymers the Kuhn length is larger than the tube diameter, $l_K \geq b$, e.g., PET and PEEK (Haward 1993) and the chain configuration between two entanglements is essentially a stiff rod instead of a random coil (Strobl 1997). The discussion regarding chain stretching is therefore not applicable to these polymer systems. Actually, the nucleation dynamics of PET is similar to the phase transition observed in liquid crystalline polymers under quiescent (Imai et al. 1992, 1993, 1995) and flowing conditions (Welsh et al. 1998, 2000). Smectic ordering is also suggested to be of importance for the nucleation of iPP by Li and de Jeu (2003).

Finally, attention is given to the development of the shish-kebab structure, which is generally believed to develop under strong chain stretching conditions, i.e., $De_s > 1$, $\lambda > \lambda^*(T)$. The strong RI may be important from the thermodynamic aspect. However, several kinetic effects may also be of relevance. First, the RI and, second, the transition from intra- to intermolecular interactions between the chain segments for $\lambda > \lambda^*(T)$ (Mavrantzas and Theodorou 1998). It is interesting to note that bundle like structures (shish) also develop in systems of associative polymers provided the flow rate exceeds the reciprocal of the characteristic time scale for the chain diffusion (Khalatur et al. 1998; Power et al. 1998). Anticipating the diffusivity on an entanglement lengthscale is more important than that of the entire chain this implies that the shish form for $De_s > 1$ (de Gennes 1982). The proposal that the 'precursor' of the shish results from the coalescence of athermal nuclei due to the applied flow field (Janeschitz-Kriegl et al. 1999) is similar in spirit, but disregards the role of the HMW chains. Experimental evidence for the importance of kinetic processes on the formation of the shish-kebab structure in iPP is given by Kumaraswamy et al. (2002) and a possible kinetic mechanism is proposed in Seki et al. (2002). On the other hand, molecular dynamic simulations on PE (Lavine et al. 2003) and experimental results on PET (Blundell et al. 1999) indicate that the nucleation is arrested during fast chain retraction, thus limiting the kinetic effects for $De_s > 1$, $\lambda > \lambda^*(T)$.

In the above it is argued that the increase of the nucleation rate due to the applied flow field can be understood from both kinetic and thermodynamic arguments. However, it is difficult to separate the individual contributions as the transitions in these processes occur at approximately identical flow conditions.

Application to flow induced crystallization experiments

In the present section the above classification of chain ordering in the different flow regimes is applied to evaluate experimental results reported in the literature. The major task is to obtain an accurate estimate of the relaxation times τ_{rep} and τ_s of the HMW tail in order to verify quantitatively which process governs the FIC dynamics. However, it turns out that it is not straightforward to identify a single, universal, procedure to determine τ_{rep} and τ_s of the chains in the HMW tail. Actually, one can propose four different procedures to do so, as discussed below. In applying these procedures one is faced with the problem that either the estimated magnitude of τ_{rep} and τ_s is not related to the HMW tail or one needs to make somewhat arbitrary assumptions to establish this relationship. (Both problems are, however, inherent to polydisperse polymer melts.) Moreover, as is shown below, the magnitudes of De_{rep} and De_s differ considerable, depending on the procedure taken, and consequently the associated mechanism which drives the FIC. This is an unsatisfactory situation and poses the major problem to be resolved in order to obtain a quantitative indication from experiments about which physical process drives FIC. In the current section different procedures are introduced to estimate τ_{rep} and τ_s, which are subsequently applied to classify FIC experiments. In the next section we discuss the advantages and disadvantages of the procedures in more detail, making use of the additional knowledge how it affects the classification of FIC experiments.

Determination of the flow regimes

Depending on the characterization of the melt with respect to the linear viscoelastic behavior or the MWD, four different procedures can be applied to estimate τ_{rep} and τ_s, which may be related to different parts of the MWD.

First, from the zero shear rate viscosity, η_0, the reptation time τ_{rep}^η follows from the relationship $\eta_0 = G_N^0 \tau_{\text{rep}}^\eta$ with G_N^0 the plateau modulus. The η_0 is known to be weakly dependent on the MWD and primarily depends on M_W (Struglinski and Graessley 1985; Berger and Meissner 1992; Aguliar et al. 2003; Vega et al. 2003; Pattamaprom and Larson 2001). Hence, the τ_{rep}^η indicates an average reptation time of the melt.

It is also possible to represent the relaxation time spectrum of the melt by a discrete spectrum of Maxwell modes (Larson 1988; Macosko 1996; Winter 1997). Despite lacking a direct relation with the MWD and the determination of the set of shear moduli G_i and reptation times τ_{rep}^i of the modes is non-unique, it gives an indication of the reptation times present in the melt (Winter 1997). Second, an average reptation time, $\bar{\tau}_{\text{rep}}$, can be obtained from the relaxation time spectrum, which is defined as $\bar{\tau}_{\text{rep}} = \sum_i G_i \tau_{\text{rep}}^i{}^2 \Big/ \sum_i G_i \tau_{\text{rep}}^i$ (Schoonen 1998). Third, the largest reptation time of the relaxation time spectrum, $\tau_{\text{rep}}^{\text{HMW}}$, can be taken which may be regarded as a measure for the HMW tail.

For the previous three procedures the magnitude of τ_s is estimated according to the relationship (Doi and Edwards 1986):

$$\tau_s = \tau_{\text{rep}}/3Z \tag{6}$$

As τ_{rep}^η, $\bar{\tau}_{\text{rep}}$ and $\tau_{\text{rep}}^{\text{HMW}}$ are not directly related to a particular chain, the magnitude of Z is somewhat arbitrary and can be taken identical to the value following from M_W, $Z_W = M_w/M_e$, or that following from the longest chains of the MWD, $Z_{\text{HMW}} = M_{\text{HMW}}/M_e$. For the procedures based on τ_{rep}^η, $\bar{\tau}_{\text{rep}}$ and $\tau_{\text{rep}}^{\text{HMW}}$ $Z = Z_W$ is taken, despite $Z = Z_{\text{HMW}}$ possibly being a more natural choice to calculate τ_s^{HMW} from $\tau_{\text{rep}}^{\text{HMW}}$.

For the final, fourth, procedure the MWD is required to obtain Z for all chains present in the melt. Subsequently, the magnitudes of $\tau_{\text{rep}}^{\text{MWD}}$ and τ_s^{MWD} follow from the relationships (Doi and Edwards 1986; Ketzmerick and Öttinger 1989)

$$\tau_{\text{rep}}^{\text{MWD}} = 3\tau_e Z^3 \left(1 - 1.51\Big/\sqrt{Z}\right)^2 \tag{7}$$

$$\tau_s^{\text{MWD}} = \tau_e Z^2 \tag{8}$$

with τ_e the equilibration time which is independent of the molecular weight of the chain (Doi and Edwards 1986; Watanabe 1999; McLeish 2002; Larson et al. 2003). This procedure is applied to estimate τ_{rep} and τ_s of the longest chains of the MWD in the next Subsection. Hence, $Z = Z_{\text{HMW}} = M_{\text{HMW}}/M_e$ with M_{HMW} the largest molecular weight of the MWD reported, which is considered to be a representative measure for the molecular weight in the HMW tail. Doing so, the effect of tube dilation and fast Rouse relaxation modes on $\tau_{\text{rep}}^{\text{MWD}}$ are disregarded for simplicity, although this is likely of importance for the HMW chains (Milner 1996; Watanabe 1999; McLeish 2002). For iPP $\tau_e = 3.54 \times 10^{-8}$ s and $M_e = 4400$ g/mol at $T = 463$ K (van Meerveld 2004b) and time-temperature superposition is applied to correct for the variation of τ_e with temperature. Similar to aPP, the magnitude of M_e varies for iPP from $M_e = 4400$ g/mol to $M_e = 5500$ g/mol at $T = 463$ K. For $M_e = 5500$ g/mol, $\tau_e = 9.87 \times 10^{-8}$ s (van Meerveld 2004b). Finally, the differences in M_e and τ_e result in a difference of τ_s^{HMW} of about a factor 1.8. However, this difference does not affect the conclusions of this paper.

The different relaxation times may be related to the melt on average, τ_{rep}^η and $\bar{\tau}_{\text{rep}}$ and, or to the HMW tail, $\tau_{\text{rep}}^{\text{HMW}}$ and $\tau_{\text{rep}}^{\text{MWD}}$. A quantitative definition of the HMW tail is not reported in the literature but a lower bound may be estimated as follows. Comparing the nuclei

density of iPP under quiescent conditions, 10^{10} m^{-3}, and flowing conditions, 10^{16} m^{-3} (van Krevelen 1978; Stadlbauer 2001; Janeschitz-Kriegl et al. 2003) with the number density of polymers, 10^{21} m^{-3}, or entanglements, 10^{23} m^{-3}, one finds that a small percentage of the MWD is sufficient to enhance the nucleation rate drastically, which is confirmed experimentally (Seki et al. 2002; Kornfield et al. 2003). (An estimate based on the observation that gelation occurs during early stages of the crystallization process (Schwittay et al. 1995; Pogodina and Winter 1998) gives a larger magnitude of the HMW tail, but this is still a small quantity of the total MWD.) These small quantities are difficult to trace down in gel permeation chromatography measurements as well as in the linear and non-linear viscoelastic regime (Eder et al. 1989; Eder and Janeschitz-Kriegl 1997; Graham et al. 2001; Seki et al. 2002; Hepperle 2002; van Meerveld 2004a). For the application of $\tau_{\mathrm{rep}}^{\eta}$, $\bar{\tau}_{\mathrm{rep}}$, and $\tau_{\mathrm{rep}}^{\mathrm{HMW}}$ two aspects are of relevance. First, the magnitude of $\tau_{\mathrm{rep}}^{\eta}$, $\bar{\tau}_{\mathrm{rep}}$, and $\tau_{\mathrm{rep}}^{\mathrm{HMW}}$ is affected by the MWD of the melt. Second, in order to determine τ_{s} via the relationship $\tau_{\mathrm{rep}}/\tau_{\mathrm{s}} = 3Z$ one is faced with the, arbitrary, choice to take Z equal to Z_{W} or Z_{HMW}, as discussed in more detail below. In view of these difficulties a direct relationship between the experimentally determined reptation times $\tau_{\mathrm{rep}}^{\eta}$, $\bar{\tau}_{\mathrm{rep}}$, $\tau_{\mathrm{rep}}^{\mathrm{HMW}}$, as well as the stretching times following from Eq. (6), and the HMW chains in the high-end tail cannot be established. The advantage of the procedure based on the MWD is that these inherent problems for polydisperse melts are resolved for the estimate of $\tau_{\mathrm{s}}^{\mathrm{MWD}}$ from Eq. (8). The assumption to neglect the effect of tube dilation and fast Rouse relaxation modes on $\tau_{\mathrm{rep}}^{\mathrm{MWD}}$, Eq. (7), may not be justified (Milner 1996; Watanabe 1999; McLeish 2002) and the magnitude of De_{rep} is expected to be overestimated.

Shear flows

For a number of experiments, reported in the literature, performed in shear flows the estimated magnitude of De_{rep} and De_{s} using the four procedures discussed in the previous Subsection are given in Table 1. The range of Deborah numbers reflects the range of shear rates covered in the experiments. It is noted that all experiments are performed, first, on iPP (although the stereoregularity is not identical), and second, at or close to a temperature of $T = 413$ K and therefore suitable to illustrate the influence of a flow field on the FIC. Time-temperature superposition is applied according to the Williams-Landel-Ferry equation specified in Swartjes (2001) for the variation of τ_{rep} and τ_{s} with T. In general, $\tau_{\mathrm{rep}}^{\eta} < \bar{\tau}_{\mathrm{rep}} < \tau_{\mathrm{rep}}^{\mathrm{HMW}} < \tau_{\mathrm{rep}}^{\mathrm{MWD}}$ and the associated magnitudes of De_{rep} and De_{s} of a flow differ by one or several orders of magnitude; see Table 1. From $\tau_{\mathrm{rep}}^{\eta}$ the magnitude of De_{rep} is in the range 0.1–10, suggesting

only orientational ordering of the chain segments governs the FIC process. This equally holds for $\bar{\tau}_{\mathrm{rep}}$, $De_{\mathrm{rep}} = 50$–1000, where, moreover, weak chain stretching may be important as $De_{\mathrm{s}} = 0.5$–10. The magnitude of De_{rep} becomes very large for $\tau_{\mathrm{rep}}^{\mathrm{HMW}}$, $De_{\mathrm{rep}} = 10^3$–10^4 and $\tau_{\mathrm{rep}}^{\mathrm{MWD}}$, $De_{\mathrm{rep}} = 10^4$–10^6, suggesting the contour path is strongly oriented. In addition (strong) chain stretching of the HMW chains can be expected as $De_{\mathrm{s}} > 1$. The magnitudes of De_{s} following from $\tau_{\mathrm{rep}}^{\eta}$ and $\bar{\tau}_{\mathrm{rep}}$ do not indicate chain stretching.

The results in Table 1 reveal that the magnitude of De_{s} is approximately identical for the procedures based on $\tau_{\mathrm{rep}}^{\mathrm{HMW}}$ and $\tau_{\mathrm{rep}}^{\mathrm{MWD}}$. It should be noted that for the calculation of $\tau_{\mathrm{s}}^{\mathrm{HMW}}$ the number of entanglements following from M_{w}, $Z_{\mathrm{W}} = M_{\mathrm{w}}/M_{\mathrm{e}}$, is taken whereas for $\tau_{\mathrm{s}}^{\mathrm{MWD}}$ that of the HMW chains, $Z_{\mathrm{HMW}} = M_{\mathrm{HMW}}/M_{\mathrm{e}}$, is considered. Despite $Z_{\mathrm{HMW}}/Z_{\mathrm{W}} = 10$–30, see Table 1, the magnitudes of $\tau_{\mathrm{s}}^{\mathrm{HMW}}$ and $\tau_{\mathrm{s}}^{\mathrm{MWD}}$ are approximately identical. This observation may be explained as follows. The difference in De_{rep} based on $\tau_{\mathrm{rep}}^{\mathrm{HMW}}$ and $\tau_{\mathrm{rep}}^{\mathrm{MWD}}$ may indicate that the magnitude of $\tau_{\mathrm{rep}}^{\mathrm{MWD}}$ reduces under the influence of tube dilation and fast Rouse relaxation modes by an order of magnitude. Hence, in reality the τ_{rep} of the HMW chains may be closer to $\tau_{\mathrm{rep}}^{\mathrm{HMW}}$ than $\tau_{\mathrm{rep}}^{\mathrm{MWD}}$. In principle, one is faced with the non-trivial task to account for the effect of tube dilation and fast Rouse relaxation modes in order to estimate $\tau_{\mathrm{s}}^{\mathrm{HMW}}$ from $\tau_{\mathrm{rep}}^{\mathrm{HMW}}$. Taking $Z = Z_{\mathrm{W}}$, instead of the more natural choice $Z = Z_{\mathrm{HMW}}$, in the relationship $\tau_{\mathrm{s}}^{\mathrm{MWD}} = \tau_{\mathrm{rep}}^{\mathrm{MWD}}/3Z$ appears to be a crude, empirical, first order correction for the effect of tube dilation, which is the reason for the approximately identical values of $\tau_{\mathrm{s}}^{\mathrm{HMW}}$ and $\tau_{\mathrm{s}}^{\mathrm{MWD}}$. As the procedure to estimate $\tau_{\mathrm{s}}^{\mathrm{MWD}}$ has a clear physical background and is not affected by the MWD, only the magnitude of De_{s} following from $\tau_{\mathrm{s}}^{\mathrm{MWD}}$ is correlated with experimental observations below.

As indicated above in shear flows the HMW chains may also reach the condition $\lambda > \lambda^*(T)$ for $De_{\mathrm{s}} > 1$ in polydisperse melts. Hence, the magnitude of De_{s} following from $\tau_{\mathrm{s}}^{\mathrm{MWD}}$ suggests that the condition $\lambda > \lambda^*(T)$ can be reached by the HMW chains present in the melt in the experiments of Liedauer et al. (1993), Vleeshouwers and Meijer (1996), Somani et al. (2000, 2001), and Nogales et al. (2001), which are discussed now in more detail. In the experiments of Nogales et al. (2001), two melts with 'short' and 'long' HMW chains, resin I and A, respectively, and blends of resin I and A are investigated at a constant shear rate and total strain. For resin I the lamellae are randomly oriented. However for the blends of resin I and A and resin A itself the lamellae are strongly oriented in the flow direction. The observation that $De_{\mathrm{s}} < 1$ for resin I and $De_{\mathrm{s}} > 1$ for resin A and the blends indicates quantitatively that the transition towards a strong orientation

Table 1 Characteristics of experiments as reported in the literature using $M_e = 4400$ g/mol and $\tau_e = 3.54 \times 10^{-8}$ s at $T = 463$ K

	Reference	M_w	PI	Z_W	Z_{HMW}	T	De_{rep}	De_s	Proc.
1	S01 (1)	500	6	113	3600	413	0.10–4.0	0.00030–0.012	η_0
2	S01 (1)	500	6	113	3600	413	56–2230	0.16–6.6	ARTS
3	S01 (1)	500	6	113	3600	413	340–13600	1.0–40	HMW
4	S01(2)	350	5.6	79	2272	413	0.063–2.5	0.00027–0.011	η_0
5	S01(2)	350	5.6	79	2272	413	12–490	0.051–2.0	ARTS
6	S01(2)	350	5.6	79	2272	413	113–4500	0.47–19	HMW
7	VM96(1)	500	6	113	3600	413	0.25–2.0	0.00073–0.0058	η_0
8	VM96(1)	500	6	113	3600	413	140–1100	0.4–3.3	ARTS
9	VM96(1)	500	6	113	3600	413	850–6800	2.5–20	HMW
10	VM96(1)	500	6	113	3600	413	34000–270000	3.3–27	MWD
11	VM96(2)	350	5.6	79	2272	413	0.080–0.63	0.00033–0.0027	η_0
12	VM96(2)	350	5.6	79	2272	413	15–120	0.064–0.51	ARTS
13	VM96(2)	350	5.6	79	2272	413	140–1100	0.59−4.7	HMW
14	VM96(2)	350	5.6	79	2272	413	8500–68000	1.3–11	MWD
15	Nea01(I)	148	4.7	34	227	423	170	0.3	MWD
16	Nea01(A)	309	7.1	70	718	423	5700	3.0	MWD
17	Sea00/01	368	4	83	1278	413	8100–83000	2.3–24	MWD
18	Lea93(3)	330	6	75	2860	416	2.1–5.1	0.011–0.023	η_0
19	Lea93(3)	330	6	75	2860	416	1900–3800	8.2–17	ARTS
20	Lea93(3)	330	6	75	2860	416	8000–16600	36–74	HMW
21	Lea93(3)	330	6	75	2860	416	0.57–1.2×10⁶	70–140	MWD
22	Lea93(3)	330	6	75	2860	423	2.5–5.2	0.011–0.023	η_0
23	Lea93(3)	330	6	75	2860	423	1900–3800	8.5–17	ARTS
24	Lea93(3)	330	6	75	2860	423	8300–16900	37–75	HMW
25	Lea93(3)	330	6	75	2860	423	0.56–1.1×10⁶	69–140	MWD
26	Lea93(3)	330	6	75	2860	430	3.9–5.2	0.017–0.022	η_0
27	Lea93(3)	330	6	75	2860	430	2900–3800	13–17	ARTS
28	Lea93(3)	330	6	75	2860	430	12600–16300	56–73	HMW
29	Lea93(3)	330	6	75	2860	430	0.82–1.1×10⁶	101–130	MWD
30	KF02	180	7.3	41	n/a	413	0.018–1.8	0.00015–0.015	η_0
31	KF02	180	7.3	41	n/a	413	7.5–75.0	0.061–6.1	ARTS
32	KF02	180	7.3	41	n/a	413	90–9000	0.73–73	HMW
33	LM76	n/a	n/a	n/a	n/a	394	1.0–8.0	n/c	η_0
34	NL98	n/a	n/a	n/a	n/a	413	0.032–57	n/c	η_0
35	NL98	n/a	n/a	n/a	n/a	415	0.029–52	n/c	η_0
36	NL98	n/a	n/a	n/a	n/a	417	0.026–47	n/c	η_0
37	PWS99	344	4	78	n/a	413	1.2–24	0.0051–0.10	η_0
38	PLSW01	350	4	80	n/a	421	22	0.092	η_0
39	EWWF03	171	4.2	39	n/a	418	0.055–0.55	0.00047–0.0047	η_0
40	EWWF03	300	5.8	68	n/a	418	0.22–2.2	0.0011–0.011	η_0
41	EWWF03	350	4.1	79	n/a	418	0.63–6.3	0.0027–0.027	η_0

The symbols are M_w: weight averaged molecular weight in kg/mol, PI: polydispersity index, Z_W: the number of entanglements per chain based on M_w, Z_{HMW}: number of entanglements of the HMW chains, De_{rep}: the Deborah number for the reptation process, De_s: the Deborah number for chain stretching, T: the absolute temperature in degrees Kelvin. The index in last column indicates if De_{rep} and De_s are determined with τ_{rep} and τ_s according to: η_0: the zero shear rate viscosity τ_{rep}^η, ARTS: average of the relaxation time spectrum, $\bar{\tau}_{rep}$, HMW: the longest time scale of the relaxation time spectrum, τ_{rep}^{HMW}, and MWD: based on longest chains in the MWD, τ_{rep}^{MWD}. The index in braces in the second column indicates the material investigated in the corresponding investigation: (1)

DSM13E10, (2) DSM15E10, (3) Dalphen KS10, (I) Resin I, (A) Resin A. S01: Swartjes (2001), VM96, Vleeshouwers and Meijer (1996), LM76, Lagasse and Maxwell (1976), NL98, Niehand and Lee (1998), PWS99, Pogadina et al. (1999), PLSW01, Pogodina et al. (2001), Nea01, Nogales et al. (2001), Sea00/01, Somani et al. (2000, 2001), Lea93, Liedauer et al. (1993), KF02, Koscher and Fulchiron (2002), EWWF03: Elmoumni et al. (2003). The range of Deborah numbers reflects the range of shear rates covered in the experiments. For the experiments of Liedauer et al. (1993) the shear rate at the wall of the duct is taken to estimate De_{rep} and De_s and the small variation in magnitudes of De_{rep} and De_s for different T is expected. n/a: not available, n/c: not calculated

of the lamellae in the flow direction correlates with the transition towards (strong) chain stretching conditions of the HMW chains.

The induction time of the DSM13E10 melt investigated by Vleeshouwers and Meijer (1996) is found to saturate to a constant magnitude with increasing the shear rate while maintaining the total strain fixed. The saturation of the induction time corresponds to the condition that $De_s > 9.0$. This finding is in good quantitative agreement with the experiments of Somani et al. (2000, 2001) for a different melt, subjected to a similar flow protocol, where the 'half-time for crystallization'

saturates for $De_s > 13.1$. The formation of the shish-kebab morphology for $De_s > 13.1$ is revealed by small and wide angle X-ray measurements in Somani et al. (2000, 2001).

The influence of the different flow regimes can also be illustrated for FIC experiments in channel flows. As $\dot{\gamma}$ is zero in the center and increases to a maximum at the wall, one passes through the different flow regimes. This qualitatively correlates with the characteristic layered structure of different morphologies (Liedauer et al. 1993; Jerschow and Janeschitz-Kriegl 1996, 1997; Eder and Janeschitz-Kriegl 1997; Kumaraswamy et al. 2000), which is illustrated in Fig. 2. Based on the profile of the shear rate in the duct and the estimated τ_s^{MWD} of the Dalphen KS 10 melt the transition from the spherulitic to fine grained morphology and the fine grained to shish-kebab morphology corresponds to $De_s > 9.4$ and $De_s > 18$, respectively, for $M_{HMW} = 10^{6.9}$ g/mol, and $De_s > 23.6$ and $De_s > 45.4$, respectively, for $M_{HMW} = 10^{7.1}$ g/mol; see Fig. 2. This indicates that

the shish-kebab morphology develops under strong chain stretching conditions. (The variation of M_{HMW} is justified as the MWD of Dalphen KS 10 reported in Stadlbauer 2001 is of a different batch compared to that investigated in Jerschow and Janeschitz-Kriegl 1997.)

It should be noted that taking different procedures to estimate τ_{rep} positions the same experiment in approximately one of the four different flow regimes. More important is that it indicates that either the orientational order or the RI of the chain segment governs the FIC dynamics. This difference was already encountered in the Introduction when comparing the relevant features of the model of Coppola et al. (2001) with that of Zuidema et al. (2001). Actually it is of general interest since both the orientation (Ziabicki 1976; Coppola et al. 2001; Nogales et al. 2001; Joo et al. 2002) and stretching of the chains (Flory 1947; Brochard-Wyart and de Gennes 1988; Bushman and McHugh 1996; Kulkarni and Beris 1998) play a key role in FIC models.

The experimental observation of the development of the shish-kebab structure in the experiments of Vleeshouwers and Meijer (1996), Nogales et al. (2001), Liedauer et al. (1993), and Jerschow and Janeschitz-Kriegl (1997)] corresponds to the condition $De_s > 1–10$ based on τ_s^{MWD}. This quantitatively indicates that (strong) stretching of the HMW chains, and the associated strong orientation and RI of the chain segments, governs the formation of the shish-kebab structure. This is in agreement with the observations in recent

Fig. 2 *Left*: morphology for the 'outdated' Dalphen KS 10 melt after the flow in a duct of 1 mm width at $T = 4203$ K with $\dot{\gamma} = 115$ ms^{-1} at the wall, Fig. 7 (page 75) of Jerschow and Janeschitz-Kriegl (1997). The distance from the center is indicated as y. (y = 0 in the center and y = 5 mm at the wall.) Large spherulites develop for y < 0.3 mm, followed by a fine grained layer $0.3 < y < 0.4$ mm and the shish-kebab morphology is present close to the wall, y > 0.4 mm (Jerschow and Janeschitz-Kriegl 1997). These transitions are indicated by the *horizontal dashed lines* in the *right figure*. *Right*: the magnitude of De_s for different M_{HMW} of the HMW chains: (*dash-dotted line*), $M_{HMW} = 10^{7.0}$ g/mol (*dashed line*), $M_{HMW} = 10^{7.1}$ g/mol (*full line*)
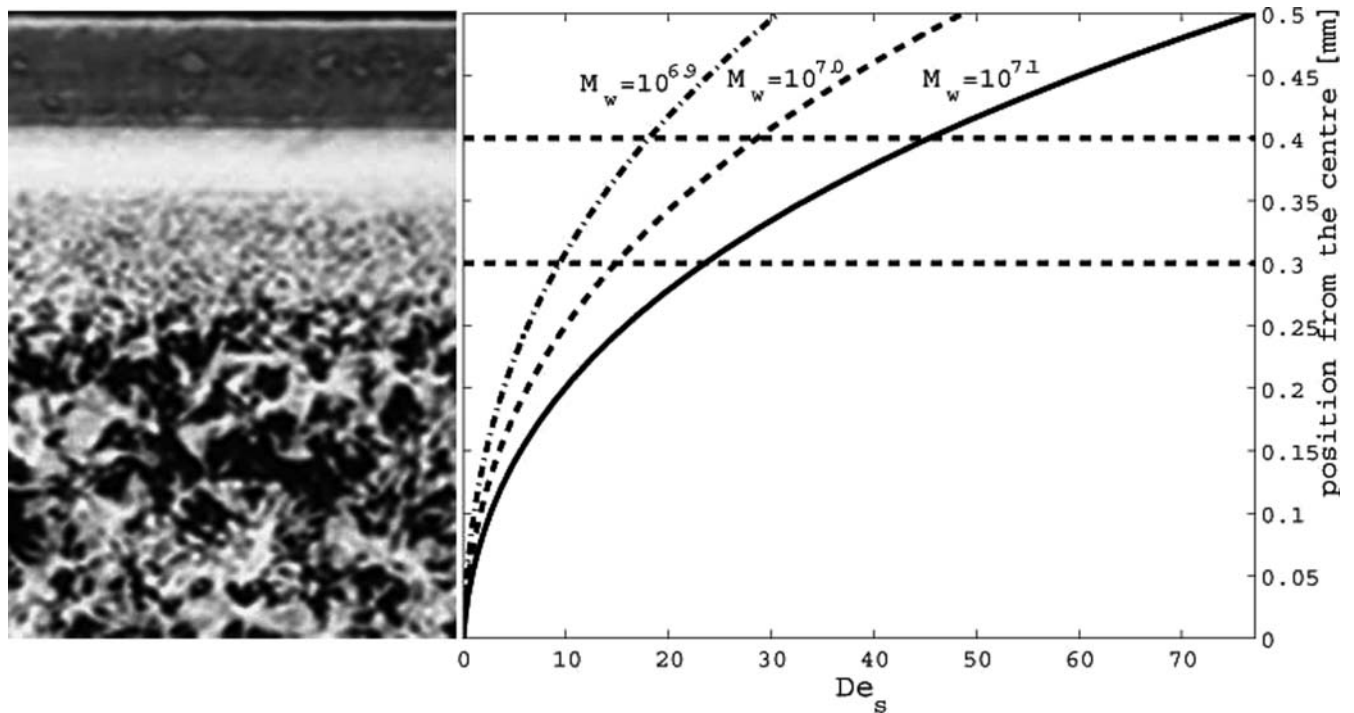
molecular dynamics simulation of PE (Dukovski and Muthukumar 2003; Lavine et al. 2003).

Extensional flows

The different flow regimes in extensional flows are illustrated for a cross-slot flow and for uniaxial extension of rubber samples.
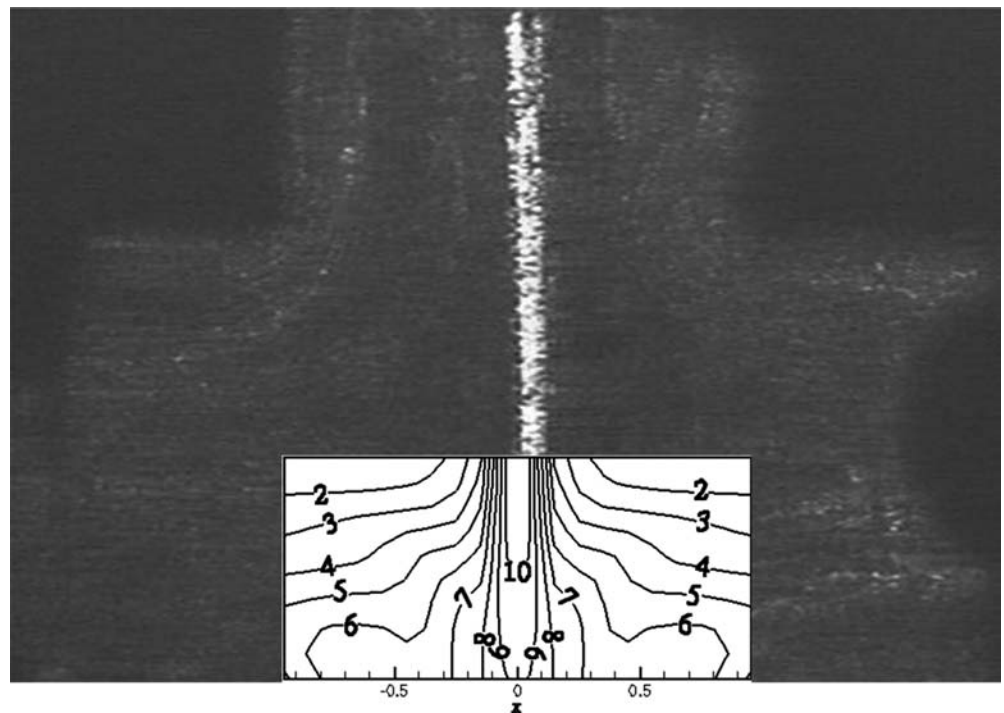
In a cross-slot flow, the majority of the flow field is a transient or stationary shear flow. Only the fluid elements on streamlines which closely approach the stagnation point in the center of the cross-slot flow are subjected to a large extensional deformation (Macosko 1996; Schoonen 1998; Verbeeten et al. 2002). Hence, the requirements $De_s > 1$ and $\lambda > \lambda^*(T)$ are most easily fulfilled by these fluid elements, being in qualitative agreement with the position where the shish-kebab morphology develops (Mackley and Keller 1973; Janeschitz-Kriegl et al. 2001; Swartjes 2001; Peters et al. 2002; Swartjes et al. 2003). The iPP melt considered by Swartjes (2001), Peters et al. (2002), and Swartjes et al. (2003) is characterized in the non-linear rheological regime, including chain stretching, and quantitatively described by a multi-mode version of the extended Pom-Pom model (Verbeeten et al. 2001, 2002; Verbeeten 2001; Swartjes 2001; Swartjes et al. 2003). The reader is referred to Verbeeten et al. (2001, 2002), Swartjes (2001), and Swartjes et al. (2003) for details about the model equations, the model parameters, the performance 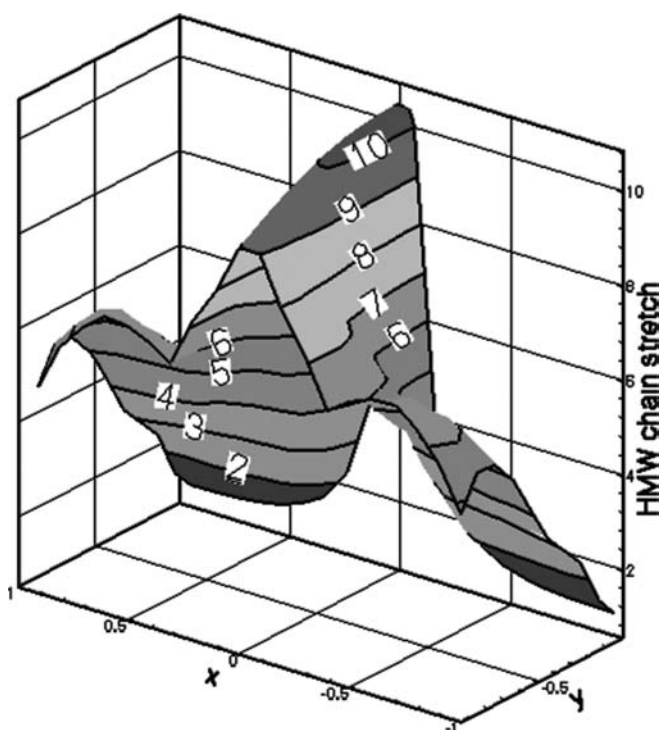in simple and complex flows, as well as the numerical implementation of the extended Pom-Pom model. Numerical simulation of the extended Pom-Pom model for this particular experiment allows one to perform a quantitative verification of the generally assumed correlation between strong chain stretching conditions of the HMW chains and the development of the shish-kebab structure (Mackley and Keller 1973; Keller and Kolnaar 1997). The chain stretch, λ, of the mode with the longest τ_{rep}^{HMW} and τ_s^{HMW} increases drastically close to the stagnation point and remains large around the centerline in the outflow channels; see Figs. 3 and 4. The position where λ is large is in agreement with the position where the shish-kebab morphology develops as revealed by birefringence; see Fig. 3. This holds equally for the wide angle X-ray diffraction measurements as presented in Fig. 5 of Peters et al. (2002) or Fig. 9 of Swartjes et al. (2003). Hence this numerical-experimental investigation provides quantitatively evidence for the correlation between the development of the shish-kebab structure and strong chain stretching conditions.

In the FIC experiments of Stadlbauer (2001) the morphology of the iPP samples remains spherulitic after the applied extensional deformation. In view of the above this may be expected as, regardless of the $\dot{\varepsilon}$, the total strain may be insufficient to reach the condition $\lambda > \lambda^*(T)$.

For the uniaxial extension of rubbers the timescales τ_{rep} and τ_s are irrelevant and the $\lambda^*(T)$ is directly related to a critical Hencky strain, ε^*, for example using the neo-Hookean theory via the relationship $\lambda = \sqrt{tr(\mathbf{B})/3}$ with $\mathbf{B}$ the Finger tensor (Macosko 1996). The Hencky

Fig. 3 Field-wise birefringence of the DSM13E10 melt at 4 min after cessation of the flow at $\dot{\varepsilon} = 0.4$ ms^{-1} at $T = 418$ K from Swartjes (2001). *Inset*: contour plot of the predicted HMW chain stretch by the extended Pom-Pom model at $T = 473$ K. Inflow in the x-direction (*horizontal*), and out flow in the y direction (*vertical*). The stagnation point is at x = 0 mm, y = 0 mm which has slightly shifted to the right after the cessation of the flow

extension of PET samples at $T = 353–363K$ (which is just above the glass transition temperature) after different quenching protocols (Salem 1992a, 1992b, 1998; Gorlier et al. 2001; Middleton et al. 2001; Marco et al. 2002a, 2002b). In general, the onset of flow induced crystallization occurs at $\epsilon \approx 2.5$. However, this strain is not identical to, first, the estimated magnitude from $\lambda^*(T)$ and, second, the strain corresponding to the experimentally measured increase of the RI of the PET chains (Middleton et al. 2001). This suggests that a critical orientation of the chain segments initializes the nucleation dynamics (Middleton et al. 2001). In addition to the experiments mentioned before (Imai et al. 1992, 1993, 1995; Welsh et al. 1998, 2000) this indicates that the crystallization dynamics of semi-flexible polymers (PET, PEN, PEEK) may be fundamentally different from that of flexible polymers (PE, iPP, PB).

Evaluation of the procedures to determine the flow regime

In the previous section four different procedures have been applied to determine τ_{rep} and τ_{s}, which in turn have been used to classify FIC experiments. However, the final magnitude of τ_{rep} and τ_{s} differ by one or multiple orders of magnitude. Consequently, this indicates that different physical processes govern the FIC dynamics. The current section is solely devoted to a detailed discussion of the four different procedures to indicate which one should be used in general.

Discussion of the different procedures to determine the reptation time and the stretching time

The analysis of the different procedures is based on two perspectives. First, are τ_{rep} and τ_{s} following from a specific procedure appropriate to characterize the ordering of the chains in the HMW tail? Second, is the magnitude of De_{rep} and De_{s} in quantitative agreement with that expected from theory?

First we start with the procedure based on the zero shear rate viscosity, $\tau_{\mathrm{rep}}^{\eta}$, τ_{s}^{η}. From experiments (see, for example, Struglinski and Graessley 1985, Berger and

Fig. 4 Surface plot of the predicted HMW chain stretch by the extended Pom-Pom model at $T = 473K$. Inflow in the x-direction and out flow in the y direction and the stagnation point is at $x = 0$ mm, $y = 0$ mm

strain is the natural logarithmic of the ratio of the current length K of the sample to the reference value, K_0, $\varepsilon = \ln(K/K_0)$. From the analysis of strain induced crystallization experiments on rubbers it follows that the strain when the oriented crystalline structure first appears in the WAXS signal, $\varepsilon_{\mathrm{FIC}}$, is approximately equal, or larger, than the magnitude of ε^* following from $\lambda^*(T)/\lambda_{\max} = 1/3$; see Table 2. This may indicate that RI is of importance for the formation of the crystallites in rubber. The variation in magnitudes of $\lambda_{\mathrm{FIC}}/\lambda_{\max}$ for the different experiments is attributed to the difference in detection limits and measurement time of synchrotron radiation (Toki et al. 2002; Murakami et al. 2002) and the device used by Toki et al. (2000).

Numerous experiments have been performed on the crystallization dynamics during and after uniaxial

Table 2 Details of several experiments, regarding the absolute Temperature T, NR: natural rubber, SR: synchrotron radiation, estimated magnitude of the maximum molecular chain stretch $\lambda_{\max}$, the Hencky strain $\varepsilon_{\mathrm{FIC}}$ when the crystallinity first appears in the WAXS pattern and λ_{FIC} the associated chain stretch based on the neo-Hookean theory

	Reference	Material	SR	T	$\lambda_{\max}$	$\varepsilon_{\mathrm{FIC}}$	λ_{FIC}	$\lambda_{\mathrm{FIC}}/\lambda_{\max}$
1	Toki et al. (2002)	NR	Yes	298	6.6	1.4	2.3	0.34
2	Murakami et al. (2002)	NR	Yes	298	6.6	1.2	2.0	0.30
3	Toki et al. (2000)	NR	No	298	6.6	1.7	3.2	0.49
4	Toki et al. (2000)	IR2000	No	298	7.8	1.8	3.5	0.45
5	Toki et al. (2000)	Cariflex	No	298	8.1	2.0	4.2	0.52

Meissner 1992, Aguliar et al. 2003, Vega et al. 2003) and theory (Pattamaprom and Larson 2001) it is known that the magnitude of η_0 is primarily related to M_w. Hence, the magnitude of τ_{rep}^{η} is an average reptation time and not that of the HMW tail. In addition one is faced with the somewhat arbitrary choice for Z to determine τ_s^{η}, using Eq. (6). Finally, the observation that $De_s < 1$ for all shear rates is in disagreement with the argument that chain stretching governs the formation of the shish-kebab structure. Hence, this indicates that the use of τ_{rep}^{η} and τ_s^{η} is inappropriate to classify a FIC experiment.

Second consider the procedure using the average reptation time from the spectrum of Maxwell modes, $\bar{\tau}_{rep}$, $\bar{\tau}_s$. Although the resulting magnitude of $\bar{\tau}_{rep}$ and $\bar{\tau}_s$ are larger than τ_{rep}^{η} and τ_s^{η} equal rheological considerations apply as for τ_{rep}^{η} and τ_s^{η}. Hence this procedure should also not be used to analyze an experiment.

Third, let us discuss the procedure based on the longest relaxation time from a spectrum of Maxwell models, τ_{rep}^{HMW}, τ_s^{HMW}. In order to determine τ_{rep}^{HMW} one encounters the following experimental difficulties. First, τ_{rep}^{HMW} can only be related to the HMW chains provided the storage, G', and loss modulus, G'', are measured in the terminal regime, where $G' \propto \omega^2$ and $G'' \propto \omega$. However, the terminal regime can not always be reached for iPP (Swartjes 2001; Elmoumni et al. 2003) and PE melts (Kraft et al. 1999) containing long chains. (This problem can be resolved by performing creep experiments; Kraft et al. 1999; Gabriel and Mündstedt 2002.) Second, the contribution of the HMW tail may be screened by the remaining part of the melt (Eder et al. 1989; Suneel et al. 2003; Hepperle 2002). It should be noted that magnitude of τ_{rep} of the chains in the HMW tail is reduced through the mechanism of tube dilation and fast Rouse relaxation modes in a complicated fashion depending of the MWD (Watanabe 1999; Pattamaprom et al. 2000; Pattamaprom and Larson 2001). All these contributions are incorporated, in some way, in the magnitude of τ_{rep}^{HMW} and it is therefore expected to be a good estimate for τ_{rep} of the HMW tail. To determine τ_s^{HMW} one should, in principle, take two steps. First, correct for the effects of tube dilation and fast Rouse relaxation modes on τ_{rep}^{HMW} in order to determine the intrinsic reptation time of the HMW tail, i.e., the magnitude which follows from Eq. (7). Next, τ_s^{HMW} follows from Eq. (6) for $Z = Z_{HMW}$ with the knowledge of the intrinsic reptation time. However, the first step is difficult to make without the knowledge of the MWD (Pattamaprom and Larson 2001). Instead, τ_s^{HMW} is estimated directly from Eq. (6) by taking $Z = Z_W$, i.e., $\tau_{rep}^{HMW}/\tau_s^{HMW} = 3Z_W$. In view of the two steps which should be taken according to theory one can certainly question this approach. Alternatively, it can be reasoned that the quantitative errors made in the individual steps partly cancel, as discussed before. This is supported by the

observation that the magnitude of τ_s^{HMW} is in agreement with τ_s^{MWD}. In summary the magnitude of τ_{rep}^{HMW} is expected to be a good estimate for τ_{rep} of the chains in the HMW tail. Although the procedure to determine τ_s^{HMW} is not free of conceptual problems, they partly cancel in the final result. Hence, at least for the experiments analyzed here, it appears that the crude procedure to obtain τ_s^{HMW} gives a reasonable estimate for τ_s of the HMW tail. This is supported by the observation that, first, the transition from the spherulitic to shish-kebab structure matches with a magnitude of $De_s \approx 1$–10 and, second, that $\tau_s^{HMW} \approx \tau_s^{MWD}$. However, whether this observation applies in general remains to be seen.

Finally, we consider the procedure based on the MWD, τ_{rep}^{MWD} and τ_s^{MWD}. The major advantage is that the procedure to estimate τ_s^{MWD} surpasses the assumptions and problems encountered to determine τ_s from τ_{rep} in the other procedures. This follows from the observation that τ_s is not affected by the MWD of the system and follows directly from Eq. (8), provided τ_e and Z_{HMW} are known. A disadvantage is that the magnitude of τ_{rep}^{MWD} is expected to be larger compared to reality, as Eq. (7) does not account for tube dilation and fast Rouse relaxation modes (Doi and Edwards 1986; Ketzmerick and Öttinger 1989). Hence, the procedure based on the MWD should be followed to obtain τ_s of the chains in the HMW tail. The preference for τ_s^{MWD} is also supported by the observation that the formation of the shish-kebab structure correlates with a magnitude of $De_s \approx 1$–10. This magnitude is in quantitative agreement with the theoretical consideration, the generally accepted argument that strong chain stretching governs the formation of the shish-kebab structure as well as with observations in molecular dynamic simulations (Lavine et al. 2003).

In conclusion it appears that there is no single procedure to obtain an accurate estimate of both τ_{rep} and τ_s of the HMW tail. For τ_{rep} it is most appropriate to take τ_{rep}^{HMW} (where it should be noted that the contribution of CCR is not included in the magnitude of τ_{rep}^{HMW}), whereas for τ_s taking τ_s^{HMW} is most suitable. Despite the number of problems encountered in estimating τ_{rep} and τ_s it is encouraging that for $De_s = \tau_s^{MWD}\dot{\gamma}$ the transition from the spherulitic to shish-kebab structure occurs for $De_s \approx 1$–10. A single value of De_s may not be expected for polydisperse melts in view of the observation that also the chain stretching dynamics is affected by the MWD, as discussed above.

'Universal' behavior for any procedure for the reptation time?

In the previous Subsection the different procedures have been discussed in detail in order to identify which one is most appropriate to determine τ_{rep} and τ_s of the HMW

tail. However, observation of Table 1 reveals that the transition from the spherulitic to shish-kebab morphology is also observed at approximately identical values of De_{rep} when, consistently, using τ_{rep}^{η}, $\bar{\tau}_{rep}$, or τ_{rep}^{HMW}. This is reported previously for a more limited set of three iPP melts by Elmoumni et al. (2003) and four isotactic poly(1-butene) melts by Acierno et al. (2003). Is this now in contradiction with the general belief that the HMW tail is essential for the FIC dynamics or is this a coincidence? It appears to be a coincidence because of the following.

The 'universal' behavior in terms of De_{rep} following from τ_{rep}^{η}, $\bar{\tau}_{rep}$ or τ_{rep}^{HMW} can be understood from the observation that for the investigated iPP melts M_w/M_n is approximately constant and only M_w differs; see Table 1. This suggests that the MWD of the different iPP melts are similar in shape and the molecular weight of all chains in the melt are shifted in magnitude. As a consequence the magnitudes of τ_{rep}^{η}, $\bar{\tau}_{rep}$, and τ_{rep}^{HMW} shift with M_w, but the ratios of the different τ_{rep} remain approximately constant. Identical observations apply to the isotactic poly(1-butene) melts investigated by Acierno et al. (2003), where one observes that the ratio of $\tau_{rep}^{\eta}/\tau_{rep}^{HMW}$ is approximately constant. This may explain why changes in the crystallization behavior are observed at approximately identical values of De_{rep} when, consistently, applying τ_{rep}^{η}, $\bar{\tau}_{rep}$, or τ_{rep}^{HMW}. This procedures may fail when, first, comparing melts which have an identical M_w but a different shape of the MWD, or secondly, in investigations where a small HMW tail is added to a particular melt, as for example in the experiments of Seki et al. (2002). The procedure to determine τ_s^{MWD} based on the MWD is not subjected to these problems and, in principle, applicable to any system. In addition such experiments may reveal if the magnitude of τ_s^{HMW} and τ_s^{MWD} still coincide, as is the case for the experiments analyzed in the present paper.

Conclusion

Four different flow regimes are identified based on the orientation and stretch of the contour path and the RI of the polymer segments, respectively, and the associated influence on the kinetic and thermodynamic contribution to the flow induced crystallization (FIC) dynamics is discussed. The analysis of FIC experiments in shear and extensional flows reported in literature provides quantitative indications that, first, the HMW chains govern the FIC dynamics, second, the number density of spherulites increases for $De_s < 1$–10 and, third, the shish-kebab morphology develops for $De_s > 1$–10 based on τ_s^{MWD}. In general, the latter also implies $\lambda > \lambda^*(T)$ for the HMW chains in polydisperse melts, which may indicate that RI of the chain segments governs the formation of the shish. These findings are confirmed quantitatively for different iPP melts analyzed in simple shear flows, duct flows and by a numerical-experimental investigation for one particular experiment performed in a cross-slot flow. Based on the present analysis the question if the shish-kebab morphology develops in a complex flow thus reduces to the question if the HMW chains are subjected to the condition $De_s > 1$, based on τ_s^{MWD}, for a sufficiently long time in order to fulfill the condition $\lambda > \lambda^*(T)$.

In the analysis of FIC experiments of polydisperse melts the determination of τ_{rep} and τ_s of the HMW tail is required. However, different procedures have to be employed to obtain an estimate of both τ_{rep} and τ_s of the HMW tail, which is an inherent problem for polydisperse melts. Nevertheless the observation that the transition from the spherulitic to shish-kebab structure corresponds to $De_s = \tau_s^{MWD}\dot{\gamma} = 1 - 10$ is encouraging, given the findings from model predictions that the chain stretching dynamics of the HMW tail chain is affected by the MWD in shear flows. Contrary to shear flows the chain stretching of the HMW tail appears to be less subjected to the MWD in uniaxial flows. Therefore experiments in uniaxial flows may have a higher potential to verify the correlation between chain stretching and the formation of the shish-kebab structure. In addition the exact magnitude of $\lambda^*(T)$ is not yet resolved for T close to and below the T_m. Also experiments on melts with a different MWD may serve as a critical test to verify the presented theory. In this respect the knowledge of τ_e and M_e can assist to 'design' a particular MWD, or flow field, in order to resolve the influence of the HMW tail and MWD on the formation of the shish-kebab structure experimentally.

In summary the primary advantage of the theory is that it provides quantitative measures which separate the degree of ordering of the chains in a particular flow field. Despite difficulties in determining τ_{rep} and τ_s of the HMW tail the comparison with experiments indicate that it captures the correct trends in a semi-quantitative manner. Hence, the present theory may serve as a helpful guideline to perform experiments in the future.

References

Abe Y, Flory PJ (1970) Rotational isomerization of polymer chains by stretching. J Chem Phys 42:2814–2820

Acierno S, Palomba B, Winter HH, Grizzuti N (2003) Effect of molecular weight on the flow-induced crystallization of isotactic poly(1-butene). Rheol Acta 42:243–250

Aguilar M, Vega JF, Peña B, Marínez-Salazar J (2003) Novel features of the rheological behavior of metallocene catalyzed atactic polypropylene. Polymer 44:1401–1407

Astarita G (1979) Objective and generally applicable criteria for flow classification. J Non-Newtonian Fluid Mech 6:69–76

Berger L, Meissner J (1992) Linear viscoelasticity, simple and planar melt extension of linear polybutadienes with bimodal molar mass distributions. Rheol Acta 31:63–74

Blundell DJ, Oldman RJ, Fuller W, Mahendrasingam A, Martin C, MacKerron DH, Harvie JL, Riekel C (1999) Orientation and crystallisation mechanisms during fast drawing of poly(ethylene terephthalate). Polym Bull 42:357–363

Brochard-Wyart F, de Gennes PG (1988) Sègrègration par traction dans un homopolymere. C R Acad Sci Paris II 306:699–702

Bushman AC, McHugh AJ (1996) A continuum model for the dynamics of flow-induced crystallization. J Polym Sci B Polym Phys 34:2393–2407

Cail JI, Stepto RFT, Taylor DJR, Jones RA, Ward IM (2000) Further computer simulation studies of the orientational behavior of poly(ethylene terephthalate) chains. Phys Chem Chem Phys 2:4361–4367

Coppola S, Grizzuti N, Maffettone PL (2001) Microrheological modeling of flow-induced crystallization. Macromolecules 34:5030–5036

de Gennes PG (1982) Kinetic of diffusion-controlled processes in dense polymer systems. II. Effect of entanglements. J Chem Phys 76:3322-3326

Debenedetti PG (1996) Metastable liquids. Princeton University Press, Princeton

Doi M, Edwards SF (1986) The theory of polymer dynamics. Claredon Press, Oxford

Dressler M (2000) The dynamical theory of non-isothermal polymeric materials. PhD thesis, ETH Zürich, Switzerland

Dukovski I, Muthukumar M (2003) Langevin dynamics simulations of early stage shish-kebab crystallization in extensional flow. J Chem Phys 118:6648–6655

Eder G, Janeschitz-Kriegl H (1997) In: Meijer HEH (ed) Crystallization. Mater Sci Technol 18:269–342

Eder G, Janeschitz-Kriegl H, Liedauer S, Schausberger A, Stadlbauer W, Schindlauer G (1989) The influence of molar mass distribution on the complex moduli of polymer melts. J Rheol 33:805–820

Elmoumni A, Winter HH, Waddon AJ, Fruitwala, H (2003) Correlation of material and processing time scales with structure development in isotactic polypropylene crystallization. Macromolecules 36:6453–6461

Fang J, Kröger M, Öttinger HC (2000) A thermodynamically admissible reptation model for fast flow of entangled polymer. II. Model predictions for shear and extensional flows. J Rheol 44:1293–1317

Flory PJ (1947) Thermodynamics of crystallization in high polymers. J Chem Phys 15:397–408

Flory PJ (1989) Statistical mechanics of chain molecules. Hanser Publisher, Münich

Gabriel C, Mündstedt H (2002) Influence of long-chain branches in polyethylenes on linear viscoelastic flow properties in shear. Rheol Acta 41:232–244

Gorlier E, Haudin JM, Billon N (2001) Strain-induced crystallization in bulk amorphous PET under uni-axial loading. Polymer 42:9541–9549

Graham RS, McLeish TCB, Harlen OG (2001) Using the Pom-Pom equations to analyze polymer melts in exponential shear. J Rheol 45:275–290

Gunton JD (1999) Homogeneous nucleation. J Stat Phys 95:903–923

Haward RN (1993) Strain hardening of thermoplastics. Macromolecules 26:5860–5869

Hepperle J (2002) Einfluss der molekularen Struktur auf rheologische Eigenschaften von polystyrol-und polycarbonatschmelzen. Ph.D thesis, Universität Erlangen-Nürnberg

Ianniruberto G, Marrucci G (1996) On compatibility of the Cox-Merz rule with the model of Doi and Edwards. J Non-Newtonian Fluid Mech 65:241–246

Imai M, Mori K, Mizukami T, Kaji K, Kanaya T (1992) Structural formation of poly(ethylene terephthalate) during the induction period of crystallization. 1. Ordering structure appearing before crystal nucleation. Polymer 33:4451–4462

Imai M, Kaji K, Kanaya T (1993) Orientation fluctuations of poly(ethylene terephthalate) during the induction period of crystallization. Phys Rev Lett 71:4162–4165

Imai M, Kaji K, Kanaya T, Sakai Y (1995) Ordering process in the induction period of crystallization of poly(ethylene terephthalate). Phys Rev B 52:12696–12704

Islam MT, Archer LA (2001) Nonlinear rheology of highly entangled polymer solution in start-up and steady shear flow. J Polym Sci B Pol Phys 39:2275–2289

Islam MT, Sanchez-Reyes J, Archer LA (2003) Step and steady shear responses of nearly monodisperse highly entangled 1,4-polybutadiene solutions. Rheol Acta 42:191–198

Janeschitz-Kriegl H, Ratajski E, Wippel H (1999) The physics of athermal nuclei in polymer crystallization. Colloid Polym Sci 277:217–226

Janeschitz-Kriegl H, Wippel H, Lin JP, Lipp M (2001) On the kinetics of polymer crystallization in opposite-nozzle flow. Rheol Acta 40:248–255

Janeschitz-Kriegl H, Ratajski E, Stadlbauer M (2003) Flow as an effective promoter of nucleation in polymer melts: a quantitative evaluation. Rheol Acta 42:355–364

Jerschow P, Janeschitz-Kriegl H (1996) On the development of oblong particles as precursors for polymer crystallization from shear flow: origin of the so-called fine grained layers. Rheol Acta 35:127–133

Jerschow P, Janeschitz-Kriegl H (1997) The role of long molecules and nucleation agent in shear induced crystallization of isotactic polypropylenes. Int Polym Proc 12:72–77

Joo YL, Sun J, Smith MD, Armstrong RC, Brown RA, Ross RA (2002) Two-dimensional numerical analysis of non-isothermal melt spinning with and without phase transition. J Non-Newtonian Fluid Mech 102:37–70

Keller A, Kolnaar HWH (1997) In: Meijer HEH (ed) Flow induced orientation and structure formation. Mater Sci Technol 18:189–268

Ketzmerick R, Öttinger HC (1989) Simulation of a non-Markovian process modelling contour length fluctuation in the Doi-Edwards model. Continuum Mech Thermodyn 1:113–124

Khalatur PG, Khokhlov AR, Mologin DA (1998) Simulation of self-associating polymer systems. I. Shear induced structural changes. J Chem Phys 109:9602–9613

Kornfield JA, Kumaraswamy G, Issaian AM (2003) Recent advances in understanding flow effects on polymer crystallization. Ind Eng Chem Res 41:6383–6392

Koscher E, Fulchiron R (2002) Influence of shear on polypropylene crystallization: morphology development and kinetics. Polymer 43:6931–6942

Kraft M, Meissner J, Kaschta J (1999) Linear viscoelastic characterization of polymer melts with long relaxation times. Macromolecules 32:751–757

Kulkarni JA, Beris AN (1998) A model for the necking phenomenon in high-speed fiber spinning based on flow-induced crystallization. J Rheol 42:971–994

Kumaraswamy G, Verma RK, Issaian AM, Wang P, Kornfield JA, Yeh F, Bhsiao BS, Olley RH (2000) Shear-enhanced crystallization in isotactic polypropylene. Part 2. Analysis of the formation of the oriented skin. Polymer 41:8931–8940

Kumaraswamy G, Kornfield JA, Yeh F, Hsiao BS (2002) Shear-enhanced crystallization in isotactic polypropylene. Part 3. Evidence for a kinetic pathway to nucleation. Macromolecules 35:1762–1769

Lagasse RR, Maxwell B (1976) An experimental study of the kinetics of polymer crystallization during shear flow. Polym Eng Sci 1:189–199

Larson RG (1988) Constitutive equations for polymer melts and solutions. Butterworths, Boston

Larson RG, Sridhar T, Leal LG, McKinley GH, Likhtman AE, McLeish TCB (2003) Definitions of entanglement spacing and time constant in the tube model. J Rheol 47:809–818

Lavine MS, Waheed N, Rutledge GC (2003) Molecular dynamics simulation of orientation and crystallization of polyethylene during uniaxial extension. Polymer 44:1771–1779

Li L, de Jeu WH (2003) Shear-induced smectic ordering as a precursor of crystallization in isotactic polypropylene. Macromolecules 36:4862–4867

Liedauer S, Eder G, Janeschitz-Kriegl H, Jerschow P, Geymayer W, Ingolic E (1993) On the kinetics of shear induced crystallization in polypropylene. Int Polym Proc 8:236–244

Mackley MR, Keller A (1973) Flow induced crystallization of polyethylene melts. Polymer 14:16–20

Macosko CW (1996) Rheology. Principles, measurements and applications. VCH Publishers, Weinheim

Marco Y, Chevalier L, Chaouche M (2002a) WAXD study of induced crystallization and orientation in poly(ethylene terephthalate) during biaxial elongation. Polymer 43:6569–6574

Marco Y, Chevalier L, Regnier G, Poitou A (2002b) Induced crystallization and orientation of poly(ethylene terephthalate) during uniaxial and biaxial elongation. Macromol Symp 185:15–34

Marrucci G (1996) Dynamics of entanglements: a nonlinear model consistent with the Cox-Merz rule. J Non-Newtonian Fluid Mech 62:279–289

Mavrantzas VG, Theodorou DN (1998) Atomistic simulation of polymer melt elasticity: calculation of the free energy of an oriented polymer melt. Macromolecules 31:6310–6332

McHugh AJ, Guy RK, Tree DA (1993) Extensional flow-induced crystallization of a melt. Colloid Polym Sci 271:629–645

McLeish TCB (2002) Tube theory of entangled polymer dynamics. Adv Phys 51:1379–1527

Mead DW, Leal LG (1995) The reptation model with segmental stretch. I. Basic equations and general properties. Rheol Acta 34:339–359

Mead DW, Larson RG, Doi M (1998) A molecular theory for fast flows of entangled polymers. Macromolecules 31:7895–7914

Middleton AC, Duckett RA, Ward IM, Mahendrasingam A, Martin C (2001) Real-time FTIR and WAXS studies of drawing behavior of poly(ethylene terephthalate). J Appl Polym Sci 79:1825–1837

Milner ST (1996) Relating the shear-thinning curve to the molecular weight distribution in linear polymer melts. J Rheol 40:303–315

Muller R, Picot C (1992) Chain conformation in polymer melts during flow as measured by small-angle neutron scattering. Makromol Chem M Symp 56:107–115

Muller R, Pesce JJ, Picot C (1993) Chain conformation in sheared polymer melts as revealed by SANS. Macromolecules 26:4356–4365

Murakami S, Senoo K, Toki S, Kohjiya S (2002) Stuctural development of natural rubber during uniaxial stretching by in situ wide angle X-ray diffraction using a synchrotron radiation. Polymer 42:2117–2120

Niehand JY, Lee LJ (1998) Hot plate welding of polypropylene. Part I. Crystallization kinetics. Polym Eng Sci 38:1121–1132

Nogales A, Hsiao BS, Somani RHM, Srinivas S, Tsou AH, Balta-Calleja FJ, Eqyuerra TA (2001) Shear-induced crystallization of isotactic polypropylene with different molecular weight distribution: in situ small- and wide-angle X-ray studies. Polymer 42:5247–5256

Oberhauser JP, Leal LG, Mead DW (1996) The response of entangled polymer solution to step changes of shear rate: signatures of segmental stretch? J Polym Sci B Polym Phys 36:265–280

Oxtoby DW (1992) Homogeneous nucleation: theory and experiments. J Phys Condens Matter 4:7627–7650

Pattamaprom C, Larson RG (2001) Predicting the linear viscoelastic properties of monodisperse and polydisperse polystyrenes and polyethylenes. Rheol Acta 40:516–532

Pattamoprom C, Larson RG, Van Dyke TJ (2000) Quantitative predictions of linear viscoelastic rheological properties of entangled polymers. Rheol Acta 39:517–531

Peters GWM, Swartjes FHM, Meijer HEH (2002) A recoverable strain based model for flow-induced crystallization. Macromol Symp 185:277–292

Pogodina NV, Winter HH (1998) Polypropylene crystallization as a physical gelation process. Macromolecules 31:8164–8172

Pogodina NV, Winter HH, Srinivas S (1999) Strain effect on physical gelation of crystallizing isotactic polypropylene. J Polym Sci B Polym Phys 37:3512–3519

Pogodina NV, Larenko VP, Srinivas S, Winter HH (2001) Rheology and structure of isotactic polypropylene near the gel point: quiescent and shear-induced crystallization. Polymer 42:9031–9043

Power D, Larson I, Hartley P, Dunstain D, Boger DV (1998) Atomic force microscopy studies on hydroxypropyl-guar gels formed under shear. Macromolecules 31:8744–8748

Salem DR (1992a) Development of crystalline order during hot-drawing of poly(ethylene terephthalate) film: influence of strain rate. Polymer 33:3182–3188

Salem DR (1992b) Development of crystalline order during hot-drawing of poly(ethylene terephthalate) film: strain-rate draw time superposition. Polymer 33:3189–3192

Salem DR (1998) Growth shape observed in two-dimensional poly(ethylene terephthalate) spherulites. Polymer 39:7067–7077

Schoonen J (1998) Determination of rheological constitutive equations using complex flows. Ph.D thesis, University of Technology Eindhoven, the Netherlands

Schwittay C, Mours M, Winter HH (1995) Rheological expression of physical gelation in polymers. Faraday Discuss 101:93–104

Seki M, Thurman D, Oberhauser J, Kornfield JA (2002) Shear-mediated crystallization of isotactic polypropylene: the role of long chain-long chain overlap. Macromolecules 35:2583–2594

Somani RH, Hsiao BS, Nogales A, Srinivas S, Tsou AH, Sics I, Balta-Calleja FJ, Ezquerra TA (2000) Structure development during shear flow-induced crystallization of i-PP: in situ small angle X-ray diffraction study. Macromolecules 33:9385–9394

Somani RH, Hsiao BS, Nogales A, Fruitwala H, Srinivas S, Tsou AH (2001) Structure development during shear flow-induced crystallization of i-PP: in situ wide angle X-ray diffraction study. Macromolecules 34:5902–5909

Stadlbauer M (2001) Rheo-kinetics of polymers in extension: rheometry, rheology, and structure development. PhD thesis, University of Linz, Austria

Strobl G (1997) The physics of polymers. Springer, Berlin Heidelberg New York

Struglinski MJ, Graessley WW (1985) Effects of polydispersity on the linear viscoelastic properties of entangled polymers. 1. Experimental observations for binary mixtures of linear polybutadiene. Macromolecules 18:2630–2643

Suneel, Graham RS, McLeish TCB (2003) Characterization of an industrial polymer melt through either uniaxial extension or exponential shear data: an application of the Pom-Pom model. Appl Rheol 13:19–25

Swartjes FHM (2001) Stress induced crystallization in elongational flow. PhD thesis, University of Technology Eindhoven, the Netherlands

Swartjes FHM, Peters GWM, Rastogi S, Meijer HEH (2003) Stress induced crystallization in elongational flow. Int Polym Proc 18:53–66

Taylor DJR, Stepto RFT, Bleackley M Ward IM (1999) A theoretical study of the conformational and orientational properties of poly(ethylene terephthalate) chains. Phys Chem Chem Phys 1:2065–2070

Toki S, Fujimaki T, Okuyama M (2000) Strain-induced crystallization of natural rubbers as detected real-time by wide angle X-ray diffraction technique. Polymer 41:5423–5429

Toki S, Sics, I, Ran S, Liu L, Hsiao BS, Murakami S, Senoo K, Kohjiya S (2002) New insights into structural development of natural rubber during uniaxial deformation by in situ synchrotron X-ray diffraction. Macromolecules 35:6578–6584

Treloar LRG (1975) The physics of rubber elasticity. Claredon Press, Oxford

van Krevelen DW (1978) Crystallinity of polymers and the means to influence the crystallization process. Chimia 32:279–294

van Meerveld J (2004a) Molecular based description of bidisperse system of entangled linear chains (preprint)

van Meerveld J (2004b) A method to extract the monomer friction coefficient from the linear viscoelastic behavior of linear, entangled polymer melts. Rheol Acta (in press)

Vega JF, Aguilar M, Marínez-Salazar J (2003) Model linear metallocene-catalyzed polyolefins: melt rheological behavior and molecular dynamics. J Rheol 47:1505–1521

Verbeeten WHM (2001) Computational polymer melt rheology. PhD thesis, University of Technology Eindhoven, the Netherlands

Verbeeten WHM, Peters GWM, Baaijens FPT (2001) Differential constitutive equations for polymer melts: the extended Pom-Pom model. J Rheol 45:823–843

Verbeeten WHM, Peters GWM, Baaijens FPT (2002) Viscoelastic analysis of complex polymer melt flows using the extended Pom-Pom model. J Non-Newtonian Fluid Mech 108:301–326

Vleeshouwers S, Meijer HEH (1996) A rheological study of shear induced crystallization. Rheol Acta 35:391–399

Watanabe H (1999) Viscoelasticity and dynamics of entangled polymers. Prog Polym Sci 24:1253–1403

Welsh GE, Blundell DJ, Windle AH (1998) A transient liquid crystalline phase as a precursor for crystallization in random co-polyester fibers. Macromolecules 31:7562–7565

Welsh GE, Blundell DJ, Windle AH (2000) A transient mesophase on drawing polymers based on polyethylene terephthalate (PET) and polyethylene naphthoate (PEN). J Mater Sci 35:5225–5240

Winter HH (1997) Analysis of dynamic mechanical data: inversion into a relaxation time spectrum and consistency check. J Non-Newtonian Fluid Mech 68:225–239

Ziabicki A (1976) Fundamentals of fiber formation. Wiley, London

Zuidema H (2000) Flow induced crystallization. Application to inject molding. PhD thesis, University of Technology Eindhoven, the Netherlands

Zuidema H, Peters GWM, Meijer HEH (2001) Development and validation of a recoverable strain based model for flow-induced crystallization of polymers. Macromol Theory Simul 10:447–460